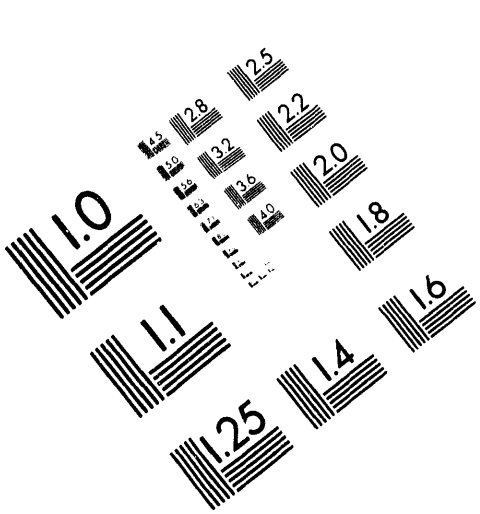

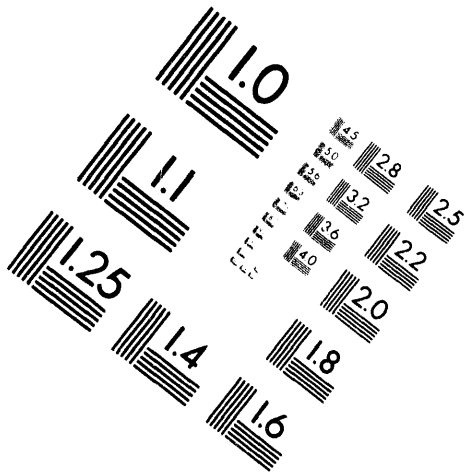

Association for Information and Image Management

1100 Wayne Avenue, Suite 1100
Silver Spring, Maryland 20910

301/587-8202

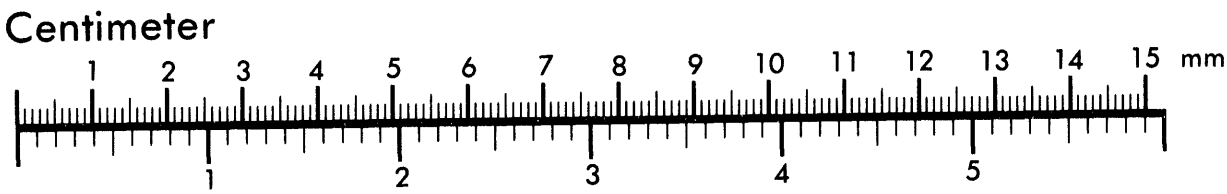

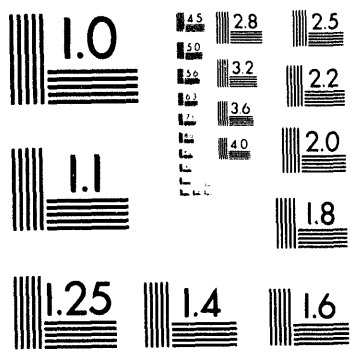

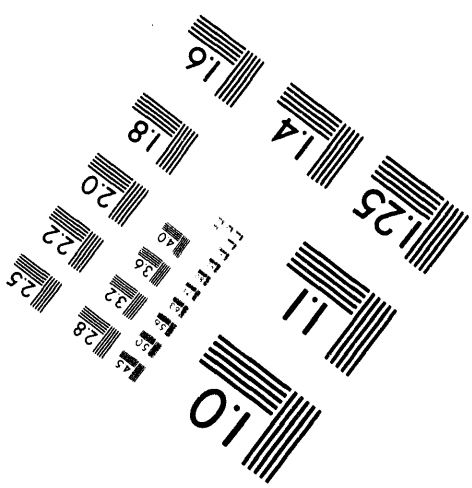

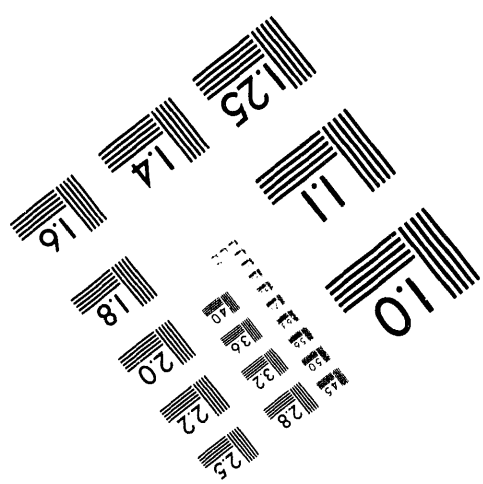

1 of 1

SOL-GEL-DERIVED SILICA FILMS WITH TAILORED MICROSTRUCTURES FOR APPLICATIONS REQUIRING ORGANIC DYES

MONICA N. LOGAN,* S. PRABAKAR** and C. JEFFREY BRINKER*,**
*Department 1846, M. S. 0607, Sandia National Laboratories, Albuquerque, NM 87185-5800
**UNM/NSF Center for Micro-Engineered Ceramics, The University of New Mexico, Albuquerque, NM 87131

ABSTRACT

A three-step sol-gel process was developed to prepare organic dye-doped thin films with tailored porosity for applications in chemical sensing and optoelectronics. Varying the acid- and base-catalyzed hydrolysis steps of sols prepared from tetraethoxysilane with identical final H_2O/Si ratios, dilution factors and pH resulted in considerably different distributions of the silicate polymers in the sol (determined by ^{29}Si NMR) and considerably different structures for the polymer clusters (determined by SAXS). During film formation these kinetic effects cause differences in the packing and collapse of the silicate network, leading to thin films with different refractive indices and volume fraction porosities. Under conditions where small pore-plugging species were avoided, the porosities of as-deposited films could be varied by aging the sol prior to film deposition. This strategy, which relies on the growth and aggregation of fractal polymeric clusters, is compatible with the low temperature and near neutral pH requirements of organic dyes.

INTRODUCTION

Organic dye-doped thin films are being developed for applications in chemical sensing [1-3] and optoelectronics [4-7]. These applications require a rigid transparent matrix so the dye can exhibit a photochromic response, a low temperature synthesis technique to prevent decomposition of the dye, and depending on the intended application, the ability to control the thin film microstructure. Porous films are useful for chemical sensing while dense films are useful for applications requiring optical, dielectric or protective functions. Sol-gel-derived inorganic glass matrices exhibit superior chemical, thermal, mechanical and optical properties compared to organic polymer matrices, can be processed at low temperatures compatible with organic dye molecules, and permit tailoring the microstructure of the matrix to the application.

Sol-gel processing offers numerous ways to control the microstructure of thin films. While there are many ways to affect the competition between phenomena that promote a more compact or a more porous structure in a dip-coated film, e.g., by changing the composition or dip-coating conditions [8-9], it is also possible to tailor the microstructure of films obtained from a single sol composition by changing the size or structure of the inorganic polymers in the sol [10-11]. Often the inorganic polymers constituting the sol are mass fractal objects, so they have two properties [12] we can exploit to tailor the microstructure of the resulting dip-coated films. First, the porosity of a mass fractal object increases with increasing size:

$$\text{Porosity} \sim \text{volume/mass} \sim r^3/r^D, \qquad (1)$$

where r = cluster size and D = mass fractal dimension ($0 < D < 3$). Second, for $D \geq 1.5$, the tendency for mass fractal objects to interpenetrate decreases with increasing size, preserving the porosity between clusters as the film is formed. Aging a sol allows the inorganic clusters to grow larger, and aging (at intermediate to basic pH) also causes the clusters to coarsen and become stiffer [13], so a film from an aged sol will have 1) more porous clusters, 2) less interpenetration of clusters as they are concentrated, and 3) less collapse of the clusters due to the capillary forces exerted during drying [8-10].

There are two complications to this simple method of varying film porosity by varying the age of the sol. First, the tendency for fractal objects to interpenetrate is a function of D as well as r.

DISCLAIMER

The tendency to interpenetrate is inversely related to the mean number of intersections $M_{1,2}$ of two mass fractal objects of size r and mass fractal dimension D placed in the same region of space [12]:

$$M_{1,2} \propto r^{(2D-3)}. \quad (2)$$

According to Equation 2, for D > 1.5, $M_{1,2}$ increases with both increasing r and increasing D, leading to a reduced tendency for interpenetration. However, Equation 1 indicates that the porosity of individual clusters increases with decreasing D. To maximize porosity, an intermediate value of D is required that balances cluster porosity and cluster-cluster interpenetration: if D is too large, individual clusters are not very porous, whereas if D is too small, cluster interpenetration reduces the porosity between clusters. We will show that D is a function of the sequence and pH of the sol preparation steps. The second complication is that small inorganic clusters can "fill-in" the pores of the deposited film, masking the porosity created by aging a sol.

EXPERIMENTAL

A two- or three-step acid/base-catalyzed process was used to prepare sols identified as B2 [10, 14-15], AAB [11], or AAB(1/5), respectively. The first step was the same for all of the sols: tetraethoxysilane (TEOS), ethanol, water and HCl were mixed in the molar ratio 1:3.8:1.0:0.007, refluxed at 60°C for 90 min and cooled to room temperature [15]. This solution, referred to as *stock solution*, was used immediately or stored in a freezer at -20°C. For B2 the second hydrolysis step consisted of adding an aqueous solution of 0.05 M NH_4OH in additional ethanol, resulting in a final molar ratio of 1 TEOS:48 ethanol:3.7 H_2O:0.007 HCl:0.002 NH_4OH, and a final sol pH of 5.5 as estimated using colorimetric pH indicator strips (EM Science). For AAB the second step consisted of adding 1 M HCl diluted in ethanol, resulting in a H_2O/Si ratio = 2.5, and refluxing at 60°C for 60 min. The third step consisted of adding an aqueous solution of 2 M NH_4OH diluted in ethanol, resulting in a final molar ratio of 1:48:3.7:0.028:0.05. For AAB(1/5) sols, the second step consisted of adding HCl, H_2O and ethanol and refluxing for 1 or 4 h, bringing the molar ratio to 1:20.6:2.5:0.0056. The third hydrolysis step consisted of adding 0.355 M NH_4OH in ethanol, resulting in a final molar ratio[1] of 1:30:3.7:0.0056:0.0078. *All three sols had the same final H_2O/Si ratio and pH.* The sols were aged in a Class-A (explosion-proof) oven at 50°C, and samples were removed at intervals up to the gel point or allowed to gel. The gelled samples were subjected to ultrasound to prepar sols of a consistency suitable for dip-coating. ^{29}Si NMR was employed to determine the species distribution of the solutions after each step and after aging the sols. The effects of synthesis and aging conditions on the intermediate-scale sol structure (0.5 - 30 nm) were determined by SAXS. Films were applied to Si substrates by dip-coating at rates varying from 10 to 25 cm/min in a nitrogen atmosphere. After 20 min drying under a heat lamp at 60°C, some films were supported on edge in quartz trays and fired in air at moderate temperatures (usually up to 400°C). Ellipsometry was used to determine the refractive index and thickness of the as-deposited and fired films. TGA experiments were performed on bulk B2 and AAB gels that had been dried at 50°C.

RESULTS AND DISCUSSION

Looking at film formation as the aggregation of non-interpenetrating fractal clusters, we expect that sol aging, which increases the size of the clusters, should increase film porosity and decrease refractive index. For films dip-coated from B2 sols, however, the expected effect did not appear until after heat treatment [10], as Table I shows. NMR studies [10, 16] of the B2 sols showed that about 5% Q^0 and 30% Q^1 species remain after aging. During dip-coating, these small, rather

[1] AAB(1/5) is more concentrated than B2 and AAB because it was part of a series of sols that were made more concentrated for more accurate NMR studies. AAB(1/5) will be diluted to be comparable to B2 and AAB when it is doped with organic dyes.

unreactive species fill in the pores of the network created by the non-interpenetrating clusters, so the as-deposited films show little variation in refractive index with sol age. TGA performed on a dried B2 gel [17] shows a 45% weight loss at 400°C owing to the removal of organics associated with these small unhydrolyzed or partially hydrolyzed species. Heating the films to 400°C reveals a range of porosity with sol age in the underlying network consistent with expectations from Equation 1.

Table I. Refractive indices and vol% porosities (calculated from the Lorentz-Lorenz relation [18]) for B2 and AAB films as a function of aging time normalized by the gelation time. Mass fractal dimension values are for sols aged for comparable normalized aging times.

B2 Sol:		As-deposited:		After 400°C:		AAB Sol:		As-deposited:		After 400°C:	
Normalized Aging Time	D	Refractive Index	Porosity (vol %)	Refractive Index	Porosity (vol %)	Normalized Aging Time	D	Refractive Index	Porosity (vol %)	Refractive Index	Porosity (vol %)
0.00	2.27	1.425	4.9	1.369	16.0	0.00	--	1.435	2.9	1.381	13.6
0.32	2.32	1.424	5.0	1.346	20.8	0.05	1.37	1.432	3.5	1.378	14.2
0.63	2.40	1.421	5.6	1.325	25.1	0.43	1.50	1.398	10.2	1.365	16.9
0.95	--	1.418	6.2	1.292	32.1	0.86	--	1.369	16.0	1.341	21.8
1.24	--	1.417	6.4	1.240	43.5	0.90	1.70	1.353	19.3	1.331	23.9

Because such a heat treatment is destructive to organic dyes, we added a second acid-catalyzed hydrolysis step (the AAB sol) to promote more complete reaction and to reduce the proportion of small, incompletely-hydrolyzed species. NMR studies of the AAB sols [16] showed that the second acid-catalyzed step promotes extensive hydrolysis and condensation: there were two broad peaks attributable to Q^2 and Q^3. The third (base-catalyzed) step promotes further condensation, and a magic angle spinning spectrum of an AAB gel 20 h after the third step shows 60% Q^3 and 40% Q^4 species. The TGA trace for a dried AAB gel [17] shows only about 20% weight loss at 400°C, and the as-deposited AAB films show the expected range in refractive index with sol age (Table I). Heating the AAB films to 400°C produces a small additional increase in porosity.

The values of the mass fractal dimension (obtained from SAXS [16]) show how the structure of the silicate polymers in the sol varies with the different routes these sols take to the same final dilution, H_2O/Si ratio and pH. The mass fractal dimensions are considerably different. We would expect AAB, which is right at the borderline of D = 1.5 for Equation 2, to exhibit different behavior than B2 with D = 2.3. However, Table I shows that both sols exhibit an increase in porosity with sol age (once the pore-plugging species are burned out of B2). The reason for this is the tradeoff between cluster porosity and cluster interpenetration. B2 clusters are less porous but pack less efficiently than AAB clusters. This tradeoff is illustrated schematically in Figure 1.

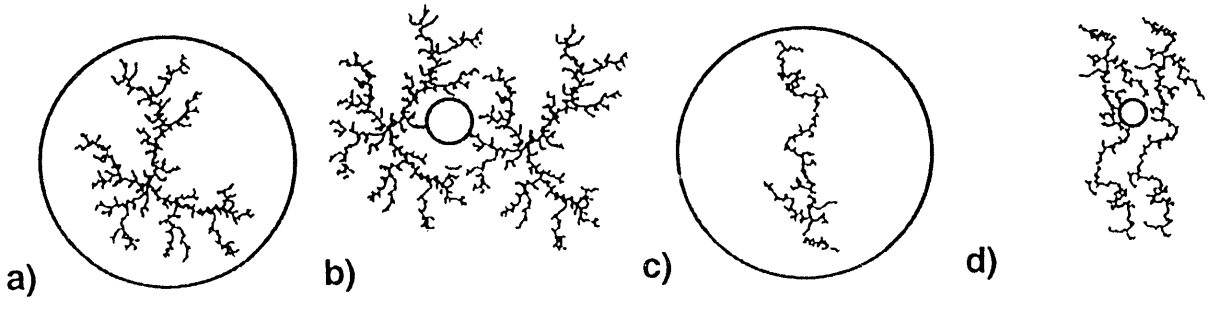

Figure 1. Schematic illustrating the tradeoff between cluster porosity and porosity between clusters with D. B2 clusters have high D: (a) individual cluster porosity is low but (b) porosity between clusters is high. AAB clusters have low D: (c) individual cluster porosity is high but (d) porosity between clusters is low.

At this point we appeared to have met our goal of being able to tailor the porosity of films from a single sol composition by a simple aging process that is carried out at temperatures compatible with organic dyes. The additional acid-catalyzed step eliminated the small pore-plugging species and the need for a heat treatment. The as-deposited AAB films showed a clear reduction in refractive index (increase in porosity) with aging, and the TGA results confirmed that organic groups were greatly reduced in AAB. Unfortunately, some of the dried AAB gels were coated with a white powder. XRD analysis [19] confirmed our suspicion that the powder was NH_4Cl salt formed from the large amounts of HCl and NH_4OH catalysts. XRD of the films showed that they were amorphous, but films that were dried at 50°C for the same period of time as the gels had loose white powder on the surface that looked crystalline under an optical microscope (30x).

Heating the films may be a simple way to remove the salt. Additional XRD studies showed that washing an AAB gel with ethanol eliminates the salt, so washing the films might also work. It would be better, however, if we found the minimum catalyst level that eliminates the small pore-plugging species. A new sol with less catalyst might also have D values that fall between those of B2 and AAB, and an intermediate value of D should produce more porous as-deposited films.

We prepared a series of sols from the stock solution with various fractions of the total moles of HCl in AAB. The base-catalyzed step was adjusted to produce a final pH of 5.5 for each sol. For sols with [HCl] = 1/4 or more of the [HCl] in AAB, XRD detected the presence of NH_4Cl in the dried gels. For sols with [HCl] = 1/10 of the [HCl] in AAB, the XRD was amorphous, the NMR showed mainly $Q^2{}_4$ cyclics, and sols at pH 5.5 did not gel after 24 days at 50°C. For sols with [HCl] = 1/5 of the original AAB, the XRD was amorphous, and the sols gelled in less than a week. After the second acid-catalyzed step, which was refluxed for 1 h, the NMR showed 17% Q^1, 62% Q^2 and 21% Q^3, and the Q^1 species were more fully hydrolyzed than in B2 sols. After the base-catalyzed step, AAB(1/5) had 24% Q^2, 49% Q^3 and 27% Q^4 species.

Preliminary refractive index data for AAB(1/5) show some dependence of refractive index on sol age, consistent with the trends observed for AAB, but a much stronger dependence on the substrate withdrawal rate. Normally, if the condensation rate is high, we would expect a faster withdrawal rate to produce more porous films. A fast withdrawal rate leads to a thicker film due to the balance between the viscous drag and the force of gravity [8-9]. Thicker films take longer to dry, so more condensation reactions can occur. This strengthens the film, making it more able to resist collapse due to capillary pressure during drying, so thicker films tend to be more porous as is generally observed for the AAB(1/5) series of films. We found that the withdrawal rate had no significant impact on the refractive index of B2 films [10], however. One possible explanation is that B2 has a large proportion of small, mainly unhydrolyzed species. (High resolution ^{29}Si NMR studies indicate that about 75% of the Q^1 species are unhydrolyzed dimer [20]). The small, unreactive, fully-ethoxylated clusters in B2 may interfere with condensation. Figure 2 shows the dependence of refractive index on withdrawal rate for AAB(1/5) as well as an upward trend for the refractive index at high ages that we cannot explain yet. Preliminary SAXS results indicate that we may not have the intermediate value of D that we hoped to achieve, so further adjustments to the process for AAB(1/5) may be needed.

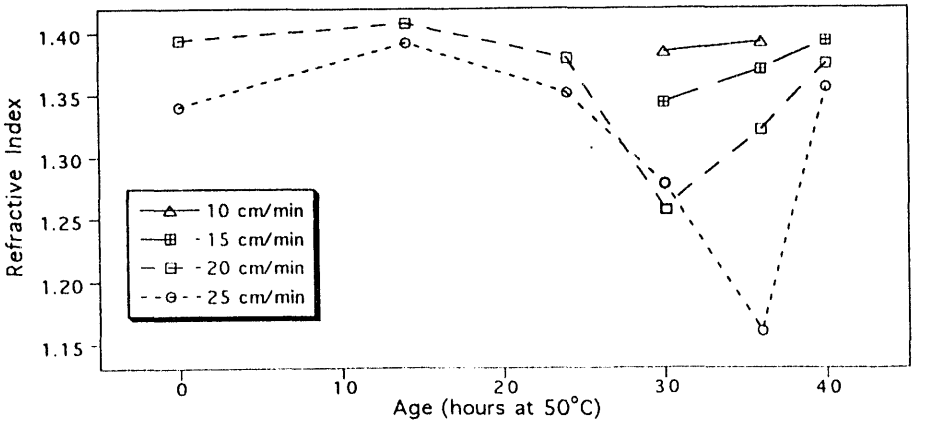

Figure 2. Preliminary refractive index data for the AAB(1/5) films.

What we have learned so far from B2, AAB and AAB(1/5) is that for sols with almost identical ingredients the sequence and timing of steps are important. This implies that kinetics determine the outcome. To test this, we prepared sols with compositions identical to AAB(1/5) but varying the order and timing of steps. Figure 3 compares the NMR spectrum for an AAB(1/5) sol to the spectra of two sols with identical composition. One sol was made by reversing the order of the second and third steps; the other was made by adding all of the ingredients in one step. In both cases, we found that at the moderate H_2O/Si ratio of 3.7, the differences from changing the order of the steps could not be erased, even after 15 h of refluxing.

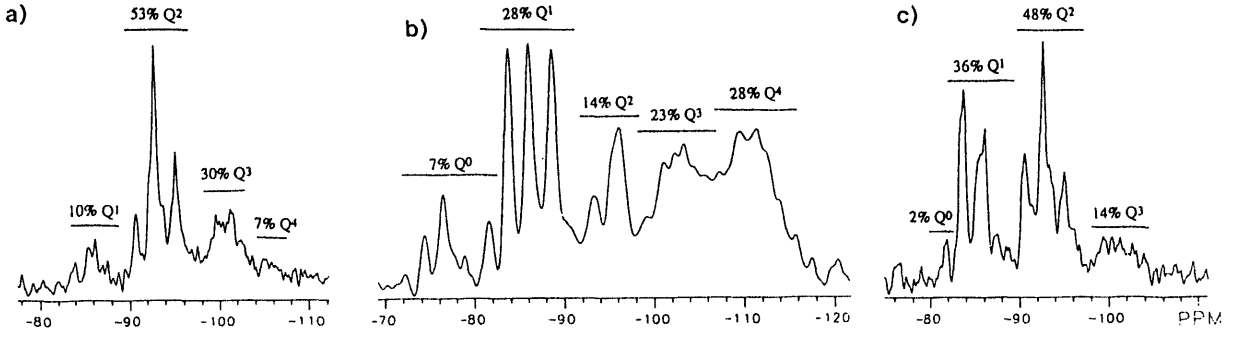

Figure 3. ^{29}Si NMR spectra of (a) an AAB(1/5) sol, (b) a sol with identical composition made by reversing the order of the second and third steps, and (c) a sol with identical composition made all in one step. The sols with differences in the timing and order of steps were refluxed for 15 h before the spectra were taken.

Next, we examined the effects of aging and refluxing between steps. We have found that stock solutions continue to age during storage at -20°C. Figure 4 compares the NMR spectrum of a freshly-made stock solution to that of a two year old stock solution. Figures 4c and 4d show the corresponding spectra recorded after adding H_2O and HCl in the second step of the AAB(1/5) process. In this case, at a lower H_2O/Si ratio of 2.5, refluxing for 4 h eliminates differences arising from the different aging histories.

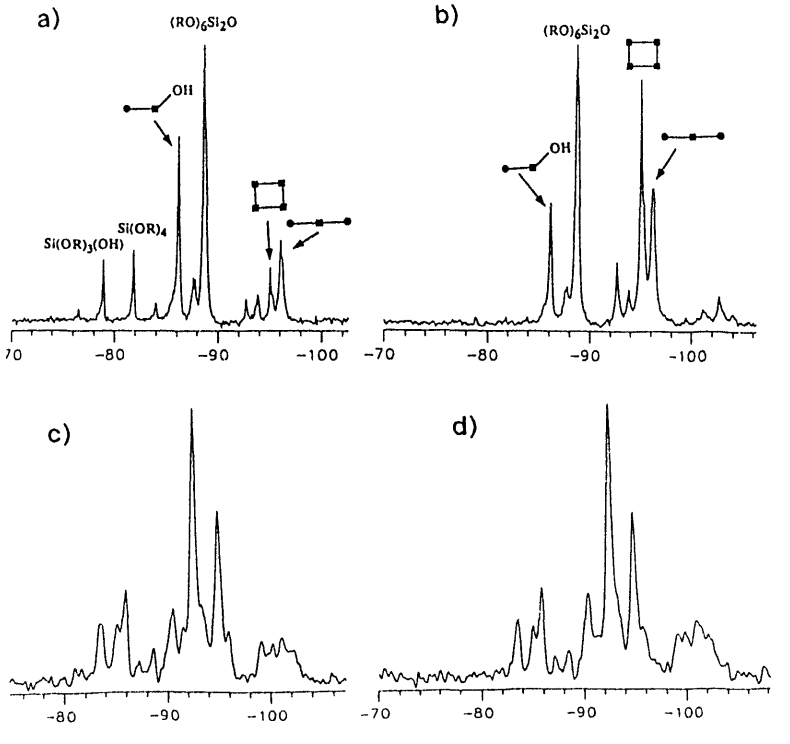

Figure 4. ^{29}Si NMR spectra for (a) freshly-made stock solution, (b) stock solution that was stored in a freezer for two years, and after 4 h refluxing of the second acid-catalyzed step of sols made from (c) the freshly-made stock, and (d) the two year old stock solution.

SUMMARY

A multi-step hydrolysis procedure was used to produce sols with fractal inorganic clusters. The sequence and timing of the steps influence the distribution of the silicate polymers in the sol and the structure of the polymer clusters. At a low H_2O/Si ratio of 2.5, these kinetic differences can be overcome by extensive refluxing of the next step. However, differences between sols at moderate water ratios persist, even after long periods of refluxing. The profound differences in the species distributions of sols prepared with the same H_2O/Si ratio, pH and concentration, but with a different sequence of steps permit kinetic control over the final film microstructure. This ability to "tune" the refractive index by a simple aging process should allow the rational design of porous films for applications requiring organic dyes.

ACKNOWLEDGMENTS

This work was performed at Sandia National Laboratories, supported by the U. S. Department of Energy under Contract # DE-AC04-94AL85000.

REFERENCES

1. D. Avnir, S. Braun, O. Lev and M. Ottolenghi in Sol-Gel Optics II, edited by J.D.Mackenzie (SPIE Proc. **1758**, Bellingham, WA, 1992) pp. 456-463.
2. O. Lev, B.I. Kuyavskaya, et al. in Environmental Monitoring, edited by T. Vo-Dink (SPIE Proc. **1716**, Bellingham, WA, 1992).
3. B. Iosefzon-Kuyavskaya, I. Gigozin, et al., J. Non-Cryst. Solids **147-148**, 808-812 (1992).
4. P.N. Prasad in Sol-Gel Optics, edited by J.D. Mackenzie and D.R. Ulrich (SPIE Proc. **1328**, Bellingham, WA, 1990) pp. 168-173.
5. R. Reisfeld in Sol-Gel Science and Technology, edited by M.A. Aegerter, M. Jafelicci Jr., et al. (World Scientific, Singapore, 1989) pp. 323-345.
6. B. Dunn, J.D. Mackenzie, J.I. Zink and O.M. Stafsudd in Sol-Gel Optics, edited by J.D. Mackenzie and D.R. Ulrich (SPIE Proc. **1328**, Bellingham, WA, 1990) pp. 174-182.
7. D. Levy, S. Einhorn and D. Avnir, J. Non-Cryst. Solids **113**, 137-145 (1989).
8. C.J. Brinker, G.C. Frye, A.J. Hurd and C.S. Ashley, Thin Solid Films **201**, 97-108 (1991).
9 C.J. Brinker, A.J. Hurd, G.C. Frye, P.R. Schunk and C.S. Ashley, J. of the Ceram. Soc. of Japan **99** (10), 862-877 (1991).
10. D.L. Logan, C.S. Ashley and C.J. Brinker in Better Ceramics Through Chemistry V, edited by M. Hampden-Smith, W.G. Klemperer and C.J. Brinker (Mat. Res. Soc. Proc. **271**, Pittsburgh, PA, 1992) pp. 541-546.
11. D.L. Logan, C.S. Ashley, R.A. Assink and C.J. Brinker in Sol-Gel Optics II, edited by J.D. Mackenzie (SPIE Proc. **1758**, Bellingham, WA, 1992) pp. 519-528.
12. B.B. Mandelbrot, The Fractal Geometry of Nature (W.H. Freeman, New York, 1983).
13. C.J. Brinker and G.W. Scherer, Sol-Gel Science (Academic Press, San Diego, CA, 1990) pp. 360-370 and 799-811.
14. C.J. Brinker, K.D. Keefer, D.W. Schaefer and C.S. Ashley, J. Non-Cryst. Solids **48** (1), 47-64 (1982).
15. C.J. Brinker, K.D. Keefer, et al., J. Non-Cryst. Solids **63**, 45-59 (1984).
16. C.J. Brinker, N.K. Raman, D.L. Logan, R. Sehgal, T.L. Ward, S. Wallace and R.A. Assink, Polymer Preprints **34** (1), 240-241 (1993).
17. D.C. Goodnow and M.N. Logan, unpublished results.
18. M. Born and E. Wolf, Principles of Optics (Pergamon, New York, 1975) p. 87.
19. M. Gonzales and M.N. Logan, unpublished results.
20. D.H. Doughty, R.A. Assink and B.D. Kay in Silicon-Based Polymer Science: A Comprehensive Resource, edited by J.M. Zeigler and F.W.G. Fearon (Amer. Chem. Soc. Advances in Chemistry Series No. 224, 1990) pp. 241-250

DATE
FILMED
10/13/94
END